2-1-2014

The Influence of Recurrent Modes of Climate Variability on the Occurrenceof Winter and Summer Extreme Temperatures over North America

Paul C. Loikith
Portland State University

Anthony J. Broccoli
Rutgers University

Citation Details

Loikith, P. C., & Broccoli, A. J. (2014). The Influence of Recurrent Modes of Climate Variability on the Occurrence of Winter and Summer Extreme Temperatures over North America. Journal Of Climate, 27(4), 1600-1618

The Influence of Recurrent Modes of Climate Variability on the Occurrence of Winter and Summer Extreme Temperatures over North America

PAUL C. LOIKITH

Jet Propulsion Laboratory, California Institute of Technology, Pasadena, California

ANTHONY J. BROCCOLI

Department of Environmental Sciences, Rutgers University, New Brunswick, New Jersey

(Manuscript received 23 January 2013, in final form 29 July 2013)

ABSTRACT

The influence of the Pacific–North American (PNA) pattern, the northern annular mode (NAM), and the El Niño–Southern Oscillation (ENSO) on extreme temperature days and months over North America is examined. Associations between extreme temperature days and months are strongest with the PNA and NAM and weaker for ENSO. In general, the association with extremes tends to be stronger on monthly than daily time scales and for winter as compared to summer. Extreme temperatures are associated with the PNA and NAM in the vicinity of the centers of action of these circulation patterns; however, many extremes also occur on days when the amplitude and polarity of these patterns do not favor their occurrence. In winter, synoptic-scale, transient weather disturbances are important drivers of extreme temperature days; however, many of these smaller-scale events are concurrent with amplified PNA or NAM patterns. Associations are weaker in summer when other physical mechanisms affecting the surface energy balance, such as anomalous soil moisture content, also influence the occurrence of extreme temperatures.

1. Introduction

Extreme temperatures are expected to change owing to anthropogenic climate warming with an increase in the severity, frequency, and duration of extreme heat events a likely and potentially dangerous anticipated climate impact (Meehl and Tebaldi 2004; Tebaldi et al. 2006; Meehl et al. 2007, 2009). Recent extreme heat events, such as those experienced in Europe in the summer of 2003 and Russia in 2011, are examples of highly unusual occurrences that are likely to become more common in the future (e.g., Beniston 2004; Schär et al. 2004; Stott et al. 2004; Dole et al. 2011; Rahmstorf and Coumou 2011). Trends in extremes have already been observed through the analysis of extremes indices (Frich et al. 2002; Alexander et al. 2006; Griffiths and Bradley 2007) with a warming of the cold tail of the temperature distribution and an increase in warm nights being the most robust trends. Additionally, recent work has shown that much of the warming to date can be attributed to external forcing (Christidis et al. 2005, 2011; Morak et al. 2011, 2013; Zwiers et al. 2011). While changes in extreme heat will be associated with the most severe climate impacts, local circulation changes may cause an increase in extreme cold events regionally, resulting from the complicated relationship between forced changes in large-scale circulation and local infrequent events (Vavrus et al. 2006; Kodra et al. 2011). To better understand how these events will change regionally, a stronger understanding of the mechanisms associated with extreme temperatures is essential for accurate projection and interpretation of future extreme events.

Several recurrent modes of natural climate variability are associated with characteristic teleconnections that impact regional mean temperature over North America, especially in winter. The Pacific–North American (PNA) pattern is associated with geopotential height anomaly centers southwest of the Aleutian Islands, inland of the Pacific Northwest, and over the southeastern United States, which correspond to temperature anomalies of the same sign (Wallace and Gutzler 1981; Barnston and

Corresponding author address: Paul C. Loikith, Jet Propulsion Laboratory, California Institute of Technology, 4800 Oak Grove Drive, Pasadena, CA 91109.
E-mail: paul.c.loikith@jpl.nasa.gov

DOI: 10.1175/JCLI-D-13-00068.1

Livezey 1987). The El Niño–Southern Oscillation (ENSO) phenomenon has well-documented associations with regional temperature impacts across the midlatitudes including over North America (e.g., Horel and Wallace 1981; Ropelewski and Halpert 1987; Kiladis and Diaz 1989; Gershunov and Barnett 1998). The northern annular mode (NAM), also referred to as the Arctic Oscillation, is characterized by an annular structure of latitudinally stratified geopotential height anomalies of opposing sign with one band at high northern latitudes and the other over the midlatitudes. When the NAM is in the positive phase, the midlatitude westerlies are anomalously strong, inhibiting the southward penetration of surges of cold air into the continental United States. This corresponds to anomalously warm temperatures in the midlatitudes and anomalously cold temperature in the Arctic. The negative phase of the NAM consists of a similar pattern but with anomalies opposite in sign (Thompson and Wallace 1998, 2000, 2001). Recent unusually cold winters in the boreal midlatitudes (2009/10 and 2010/11) have been associated with a strong negative phase of the North Atlantic Oscillation (NAO), a pattern that is highly correlated with the NAM, consistent with a relationship between the amplitude of the pattern and the magnitude of the temperature anomalies (Guirguis et al. 2011; Wang et al. 2010; Cattiaux et al. 2010).

A number of studies suggest a strong linkage between the amplitude and phase of these recurrent circulation patterns and extreme temperatures. Significant impacts on temperature extremes are found by Higgins et al. (2002) owing to changes in the phase of ENSO and the NAM across the United States. Gershunov and Barnett (1998) show that changes in the probability of extreme temperature days in winter over the continental United States related to the phase of ENSO do not necessarily follow systematic shifts in central tendency of the temperature frequency distribution that are characteristic of ENSO. Kenyon and Hegerl (2008) also show statistically significant associations between phases of ENSO and extreme temperature days. Both of these studies show substantial nonlinearity in the response of temperature extremes to opposing phases of ENSO.

Several studies have specifically focused on the association between modes of climate variability and temperature extremes in the northeastern United States and southeastern Canada. Wettstein and Mearns (2002) show a dipole in the sign of the association between temperature extremes and the phase of the NAO/NAM. Griffiths and Bradley (2007) show that extreme warm temperatures preferentially occur during a positive phase of the NAM and extreme cold temperatures during a negative phase. Brown et al. (2010) suggest that the influence on extremes from modes of climate variability over long time periods is not robust in this region.

Loikith and Broccoli (2012, hereafter LB12) systematically identified and described the principal atmospheric circulation patterns associated with temperature extremes over North America. Their results suggest that local, transient weather patterns, generally characteristic of the synoptic scale, are the key mechanisms associated with daily temperature extremes. Such patterns were found to be especially robust in winter, while summer circulation anomalies were shown to be weaker and smaller in spatial scale. LB12 hypothesize that surface–atmosphere coupling plays an important role in the occurrence of extreme summer temperature days when a preferred circulation pattern is not evident. This work builds on the analysis of LB12 and aims to answer the question: how important is the phase of influential modes of climate variability in the occurrence of extreme temperatures over North America in relation to other, smaller-scale circulation patterns and physical processes?

The focus of this paper is on the NAM, PNA, and ENSO (using the Niño-3.4 index). The NAM and PNA were chosen because they account for the majority of the atmospheric variability in the Northern Hemisphere and both have been shown to impact North American climate (Quadrelli and Wallace 2004). ENSO is also examined separately as it has the most important influence on global climate on seasonal to interannual time scales. The association between ENSO and the PNA has been discussed at length in the literature (Straus and Shukla 2002 and references therein); however, the relationship between the two modes during the time period used in this study appears weak, so both are treated as separate phenomena. Other modes of variability with characteristic temperature teleconnections for North America were considered but are not the focus of this paper as most are either highly correlated with one of the patterns already being analyzed or are less closely associated with climate impacts over North America. For example, the NAO is an important mode of variability for portions of North American climate (Hurrell et al. 2003), but the pattern is highly correlated with the NAM. The annular nature of the NAM also has potential to impact a larger portion of the domain compared with the NAO. Data and methods are described in the next section and the associations between extreme temperatures and the NAM, PNA, and ENSO are presented in section 3. Section 4 discusses the spatial scale of circulation patterns associated with extremes and section 5 looks at the influence of surface wetness on summertime extremes. Concluding remarks follow in section 6.

2. Data and methods

a. Data

Daily temperature extremes were extracted from the HadGHCND gridded daily temperature dataset (Caesar et al. 2006), a joint collaboration between the U. K. Met Office's Hadley Centre for Climate Prediction and Research and the U.S. National Climatic Data Center (NCDC). The dataset has a resolution of 2.5° latitude by 3.75° longitude and consists largely of observations from the NCDC Global Historical Climatology Network–Daily (GHCND). The HadGHCND has two products, observed daily maximum and minimum temperatures and daily maximum and minimum temperature anomalies. The latter dataset, which spans the years 1950–2007, was used. While the HadGHCND has a global domain, only data over North America, defined here as all land north of 17.5°N between the Pacific and Atlantic Oceans, were used. The anomalies are computed by subtracting the 5-day running mean from a 30-yr climatology spanning 1961–90 from the actual temperature (Caesar et al. 2006). Composites of circulation patterns were calculated using data from the National Centers for Environmental Prediction's Reanalysis-1 (Kalnay et al. 1996), which has a slightly higher resolution than the HadGHCND dataset at 2.5° by 2.5°.

NAM and PNA index values were obtained from the Climate Prediction Center (CPC) website (http://www.cpc.ncep.noaa.gov/). The NAM index is calculated in this dataset by projecting the mean 1000-hPa height anomalies on the leading EOF of the 1000-hPa field north of 20°N. The PNA is defined using the first and second rotated empirical orthogonal functions of the 500-hPa geopotential height field following the methods of Barnston and Livezey (1987). Monthly or daily index values are obtained using least squares regression. The Niño-3.4 index data were obtained from the National Center for Atmospheric Research's Climate and Global Dynamics division and are freely available via the web (http://www.cgd.ucar.edu/cas/catalog/climind/Nino_3_3.4_indices.html) and discussed in Trenberth (1997). The Niño-3.4 index is defined as the standard deviation of the monthly sea surface temperature anomaly in the Niño-3.4 region, smoothed by a 5-month running mean. The NAM and PNA are both available as daily and monthly values while the Niño-3.4 index is only monthly. Daily temperature extremes were therefore associated with the Niño-3.4 index value of the month in which the extreme day occurred. This is a reasonable approximation because the SST anomalies that define ENSO evolve more slowly than the other two modes of variability. In the case of missing index value data, the missing days are removed from both the index value dataset and the temperature anomaly dataset. This was only an issue for a few days for the NAM in summer.

b. Methodology

Temperature extremes and composites of circulation anomalies are defined largely in the manner of LB12 except that a slightly different threshold is used. Extreme temperature days in this work are defined as those days or months falling above the 90th and below the 10th percentile in the temperature anomaly frequency distribution for the months of December–February (DJF) and June–August (JJA), representing boreal winter and summer, respectively, at each grid point. The results presented in LB12 indicate that circulation patterns associated with extremes in transition seasons had commonalities with both summer and winter, so fall and spring associations are not presented in this paper. The sample size was expanded from that used in LB12 to include 3-month datasets and the percentile threshold defining an extreme was expanded to 10% to increase the sample size for evaluating the association between extreme temperature months and the modes of variability. Daily DJF and JJA cold and warm extremes consist of 270 and 276 days, respectively, for each extreme [90 days (DJF) or 92 days (JJA) $\text{yr}^{-1} \times 30\,\text{yr} \times 0.10$]. Monthly extremes consist of nine months for both DJF and JJA ($3\ \text{months}\ \text{yr}^{-1} \times 30\,\text{yr} \times 0.10$). The sample size can be larger in the case of a tie with the 270th (276th) most extreme day or 9th most extreme month. As in LB12, the analysis was performed using the years 1961–90 (DJF is December 1960 through February 1990 to keep seasons coherent). This period was chosen as a compromise between the need for a sample size large enough to evaluate significance and the desire to reduce any long-term trend in temperature during the period of analysis.

The associations between extreme temperature days and the phase of each circulation mode were identified by calculating the percentage of extreme temperature events (i.e., warm and cold daily and monthly maximum and minimum temperature extremes) that were concurrent with index values falling in the upper or lower quartiles of the distribution. Thus, the expected percentage that would occur by chance is 25%. A percentile threshold was chosen as opposed to an index value threshold to equally represent the low and high tails of the distribution of index values, even in the case of an asymmetric distribution. Results from the same analysis with different thresholds do not yield appreciable differences in the pattern and significance of association percentage values.

Extreme temperature days often occur in series of consecutive days, so each extreme is not necessarily independent. To assess statistical significance without

assuming that the data are free of serial correlation, a Monte Carlo simulation was performed. The simulation is performed following this example: the 30-yr time series of temperature and circulation index values were divided into 30 individual 1-yr time series for each of the two variables. Next, the time series are randomly paired and the analysis described in the previous paragraph is performed. This process was repeated 10 000 times, producing a frequency distribution for the association between temperature and circulation index for randomly paired time series. The 5th and 95th percentiles of this synthetic frequency distribution are used as thresholds of statistical significance at the 5% level. This process was repeated for all three modes and for all types of temperature extremes (warm and cold, minimum and maximum) separately so that all association calculations have a confidence threshold for each grid cell.

Soil moisture reanalysis data used here is a product of the Variable Infiltration Capacity (VIC) model (Liang et al. 1994) and is available for the continental United States for the time period and resolution needed for this analysis. The limited spatial coverage is sufficient for this analysis as areas north of this region are more influenced by synoptic-scale circulation patterns in the summer than the continental United States while only a small fraction of the domain used in this paper lies to the south. The data were originally on a 0.5° by 0.5° grid, but smoothed to a 2.5° by 3.75° grid to match the HadGHCND temperature dataset. Only soil moisture amounts (in millimeters) for the topmost soil layer were used to calculate soil moisture anomalies. Anomalies were calculated relative to normal values for each day obtained using a 5-day window centered on each day of a 30-yr climatology for each day. Anomalies are expressed as percentage of normal soil moisture for each grid cell in the domain.

3. Temperature extreme–circulation index associations

In this section, daily and monthly statistical associations between extreme temperatures and the NAM, PNA, and ENSO are presented. A closer look at individual cases is also taken to investigate the influence of these circulation patterns at specific locations versus other mechanisms that may be important for the occurrence of extreme temperatures. Results for the NAM and PNA are presented separately from the ENSO analysis because the NAM and PNA are defined by anomalies in atmospheric circulation, while the ENSO index is indicative of the state of the ocean and less directly related to atmospheric circulation. While associations of all types of extremes in both seasons were examined, for brevity only DJF extreme cold minimum and JJA extreme warm maximum events are presented here as these extremes account for the most severe climate impacts. Hereafter, the use of a plus sign as a suffix (e.g., NAM+ and PNA+) indicates days when the index values are in the upper quartile (i.e., large positive) and a minus sign (e.g., NAM− and PNA−) indicates index values that are in the lower quartile (i.e., large negative). Temperature extremes are labeled as Tx90 and Tn10 for extreme warm maximum and cold minimum daily or monthly temperatures, respectively.

Statistical associations

1) PNA AND NAM

The percentage of extreme temperature days concurrent with days in the upper and lower quartiles for the NAM and PNA are plotted in Fig. 1. While a given grid cell could have an association percentage significantly lower than expected by chance (i.e., 25%), only associations significantly higher than this value at the 5% level are shaded. This method of shading emphasizes areas where there is an increased probability of extreme temperatures when the index value is outside of the indicated threshold. The color scheme is such that cold colors represent an increased probability of extreme cold temperatures during the indicated phase of the circulation pattern while warm colors represent an increased probability of extreme warm temperatures. Locations with an enhanced probability of a particular type of extreme generally have a reduced probability of that type when the mode of variability has the opposite polarity.

The PNA has the most robust association in DJF with a strong increase in the probability of extreme cold minimum temperatures over much of the western and northwestern portions of the continent during negative PNA events. Positive PNA events tend to favor extreme cold temperatures over southeastern North America. Both the northwest and southeast portions of North America are located in the vicinity of the characteristic centers of action that define the PNA. The relatively higher association values found over northwestern North America in the PNA− case when compared with southeastern North America in the PNA+ case is likely a result of the tendency for the geopotential height anomalies associated with the PNA to be stronger near northwest North America than over southeast North America. In southeastern North America, while a significant increase in the probability of extreme cold minimum temperatures is associated with highly positive PNA days, many such days (~50%) occur when the PNA is not exceeding this threshold. This suggests that the PNA, while an important influence on local daily

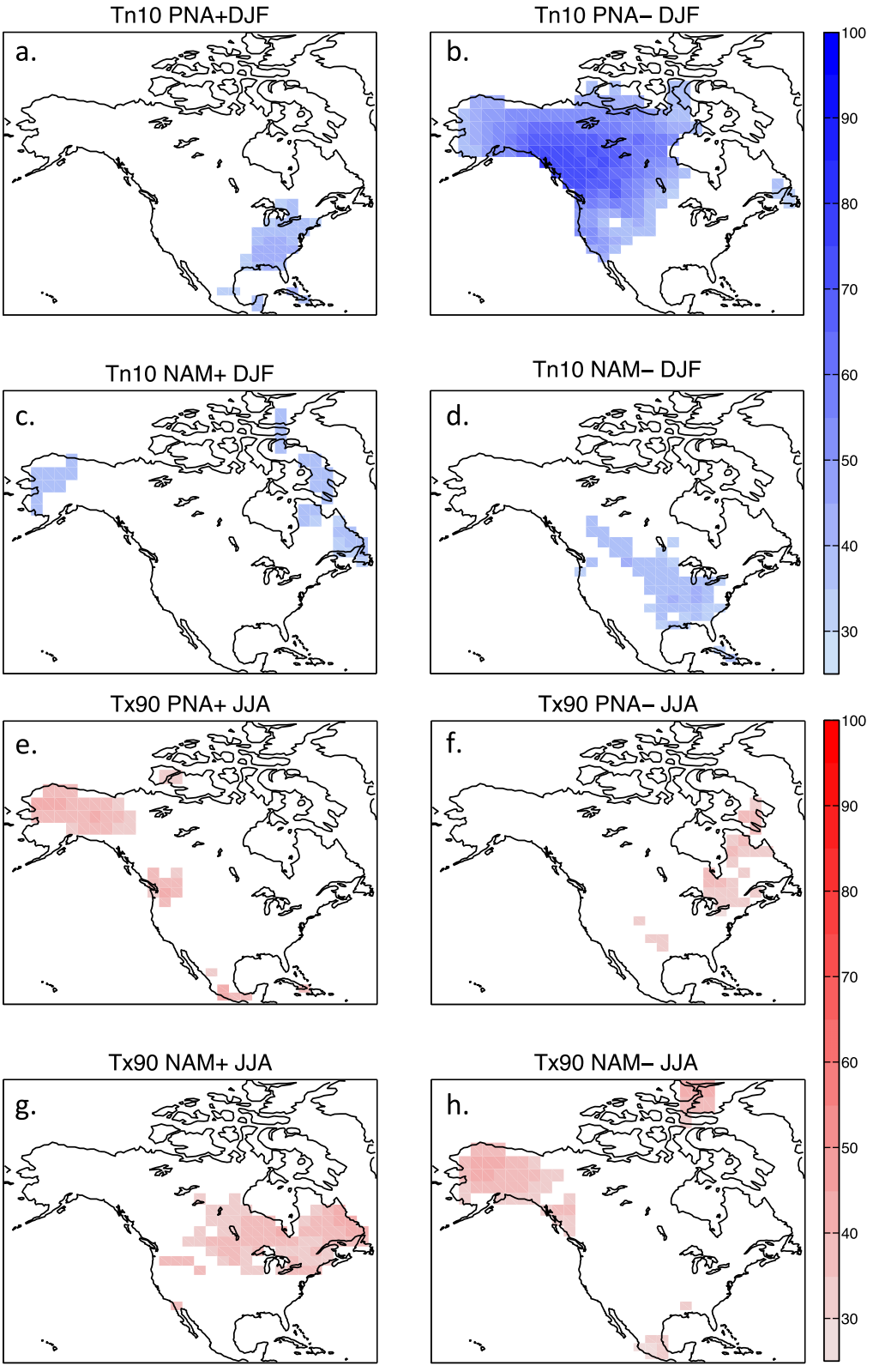

FIG. 1. The percentage of (a)–(d) extreme cold DJF minimum and (e)–(h) extreme warm JJA maximum temperature days that occur when the PNA or NAM are in the upper (+) or lower (−) quartile of the index value distribution. Only grid cells where the percentage is significantly greater than expected by chance at the 5% level are shaded.

temperature, is only one influential mechanism for this region. Association patterns and percentage values (not shown) are similar for Tx10 days while Tn90 and Tx90 association patterns are nearly opposite those for extreme cold days.

A positive NAM is associated with an increase in the probability of extreme cold minimum temperatures over the far northeast and northwest portions of the continent, where the positive phase of the NAM is associated with lower than average geopotential heights. The area of increased probability of cold events is shifted southward during negative NAM days as a weakening of the prevailing westerlies associated with the negative phase of the NAM allows colder air to penetrate equatorward. The increased probability is much lower for the NAM compared with the PNA and suggests that the NAM may be a less dominant influence in extreme daily temperatures over North America compared with the PNA. Some of the area in southeast North America that has more frequent cold days with NAM− also has more frequent cold days with PNA+. This indicates that cold extremes in this region are subject to a relatively high influence from large-scale circulation, and concurrence of modes could also be important here. Warm extremes (not shown) are more influenced by the NAM over the northeastern part of the continent than cold extremes, with the negative phase of the NAM being highly associated with extreme warm temperatures here.

Summertime associations are weaker in general, especially at lower latitudes where weak baroclinicity results in circulation patterns that are smaller in scale and weaker in magnitude than in the winter (LB12). There is an increased probability for extreme warm days over much of Alaska and northwestern Canada during both PNA+ and NAM− events. Similarly, the east-central portion of the continent has an increased probability of extreme warm days during PNA− and NAM+ days. The NAM associations in summer still suggest an annular structure with a zonal band of significant association values across much of the continent during NAM+ days. The southeast North America area of association that would be expected for the PNA− case based on the results of DJF is not present as this is likely too far south to be strongly influenced by the extratropical circulation.

Because these patterns evolve and persist over multiple days, it is of interest to examine the association between extremes in both temperature and index value on longer time scales. Figure 2 shows the same analysis, except the associations are between extremely warm and cold months and unusually positive or negative index value months. In winter, the patterns are generally similar to those in Fig. 1 except the percentages are generally higher. Nearly all months with extremely cold mean minimum temperature values occur during PNA− months over much of northwest North America, while the same is true in southeastern North America for PNA+ months. The NAM also has similarities with the daily associations but with stronger percentages for NAM+ over northeast North America and more areas of significant association that are more scattered for NAM−. Some of this scatter may be due to the relatively small sample size of months that exceed the temperature and index value threshold compared with the daily analysis.

Months with extreme warm mean maximum temperature in JJA have some commonalities with the daily associations, especially over northeastern North America for the PNA− case, Alaska for the NAM− case, and eastern Canada for the NAM+ case. There are few significant associations with PNA+ months when compared with the other association maps. The interior of the northern half of the continent is strongly associated with NAM+ months while only the southern half of this region shows comparable associations in the daily analysis. This may suggest more influence on temperature extremes over longer time scales from the NAM in north-central Canada.

Figure 3 shows the percentage of extreme temperature days that occur when neither mode is prominent, that is, for cases in which both the PNA and the NAM are in the middle half of the distribution. In this case, all associations greater than 25% (the expected probability if the association is random assuming that the PNA and NAM operate independently) are shaded in color while associations less than 25% are shaded in gray. In winter, most extreme temperature days occur when the index value of at least one pattern is in the upper or lower quartile of the distribution in most places. In the summer, a larger area of the domain experiences extreme temperatures when neither pattern is in the upper or lower quartile for the index value distribution. This emphasizes that numerous extremely warm days in the summer occur when the index value for either pattern is not unusually amplified, suggesting a weak relationship between the phase and strength of the PNA and NAM and extreme warm summer temperatures in these regions.

2) ENSO

Figure 4 shows the associations between extreme temperature events and ENSO for both daily and monthly time scales. In these maps, shading indicates associations that are stronger than would be expected by chance irrespective of statistical significance, while those grid cells with statistically significant relationships at the 5% level are highlighted. The change in plotting convention is made because of the overall

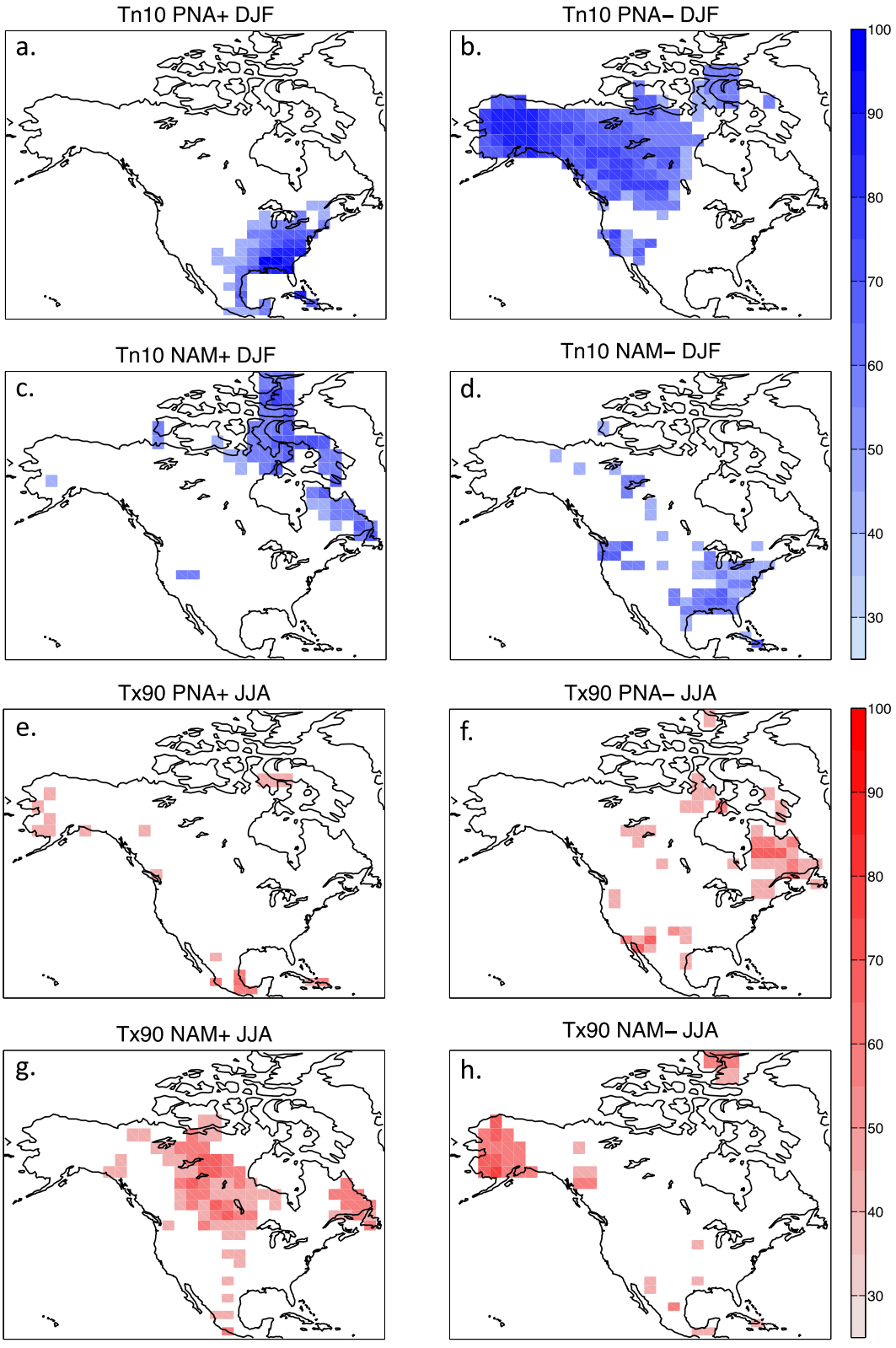

FIG. 2. As in Fig. 1, but for monthly mean temperature.

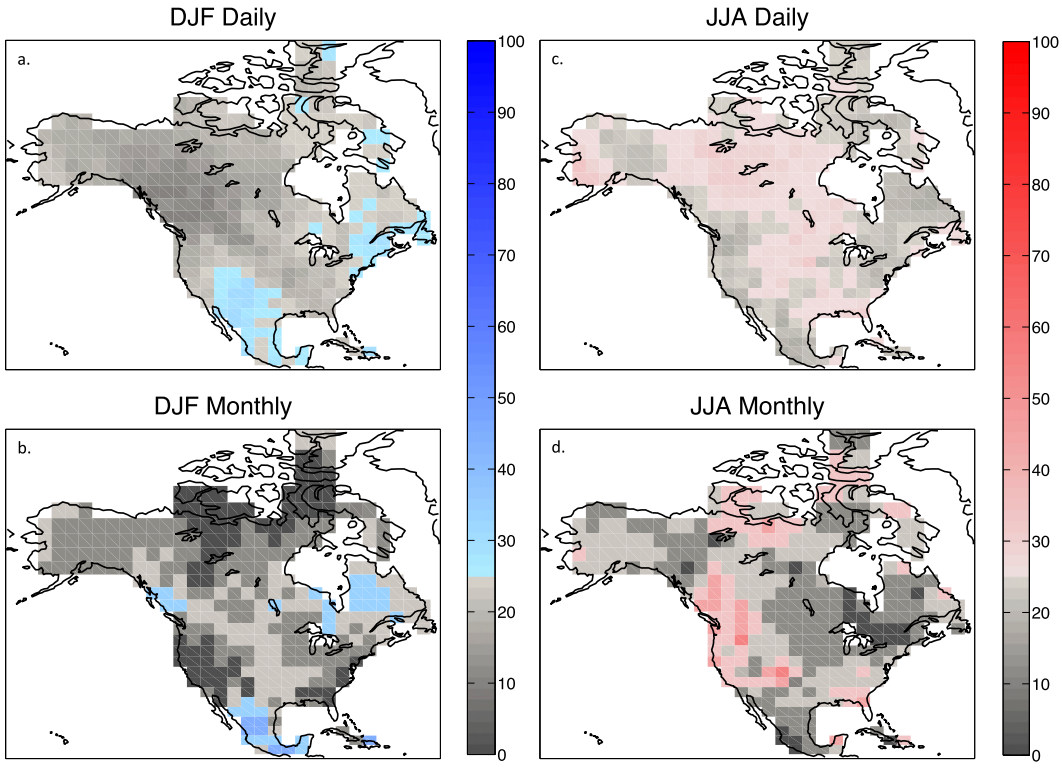

FIG. 3. The percentage of extreme cold DJF minimum temperature (a) days and (b) months and extreme warm JJA maximum temperature (c) days and (d) months that occur when neither the PNA nor the NAM is in the upper or lower quartile. Grid cells shaded in blue (red) for DJF (JJA) are where the percentage of extreme cold (warm) is greater than expected by chance (25%) when neither mode is amplified. Gray shaded grid cells are where percentages are lower than expected by chance.

small number of statistically significant grid cells in the ENSO association calculations. Overall, associations are weak, and the area of statistical significance is much less than that seen in the PNA and NAM cases. The relative weakness of the relationship between extreme temperature events and ENSO as contrasted with the results for NAM and PNA is likely due to the more direct relationship between temperature and local atmospheric circulation. Although ENSO teleconnections clearly affect atmospheric circulation, the influence on temperature is less direct than that of the other two patterns, which are defined by atmospheric circulation anomalies directly over North America. There is an increased probability of extreme cold days over much of the northern and western portions of the continent during La Niña events, but only a few grid cells in Alaska are statistically significant. Associations are generally weak for Niño+ days and months while Alaska has more statistical significance in Niño− months. There is also an increased probability of extreme cold minimum temperature months over the Rocky Mountains and over northeastern North America during Niño− months.

In JJA, the northern tier of the continent shows significantly increased probabilities of extremely warm days and months during La Niña events while Alaska tends to have an increased probability during El Niño months. Niño+ days and months are also associated with an increased probability of warm summer days and months over Mexico and the south-central United States. Places where ENSO is associated with extreme warm temperatures in the summer, especially at lower latitudes, may experience circulation patterns that inhibit precipitation and cloudiness rather than circulation that influences advection of warm air.

The relatively modest areas of significant association between ENSO and temperature in this study contrast with the results of Kenyon and Hegerl (2008), who show more widespread statistically significant associations between the sign of ENSO and extreme temperature days in their analysis of station data over North America. One aspect of the design of this study that could explain this difference is the smaller sample size of the dataset used here. Kenyon and Hegerl (2008) used available data from 1849 to 2005 while this work uses 1961–90. Another difference is that Kenyon and Hegerl

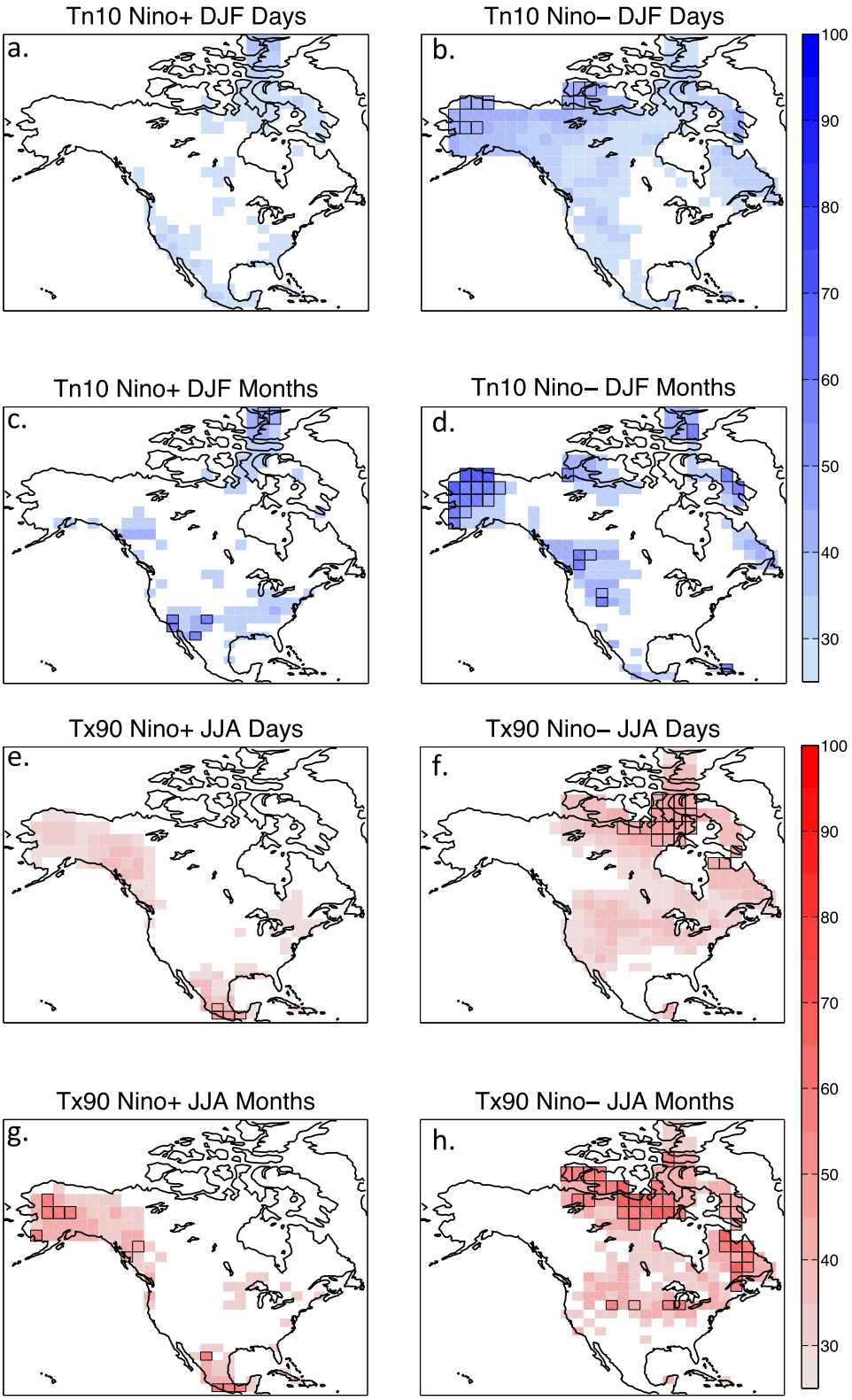

FIG. 4. The percentage of extreme cold DJF minimum temperature (a),(b) days and (c),(d) months and extreme warm JJA maximum temperature (e),(f) days and (g),(h) months that occur when the Niño-3.4 index is in the upper or lower quartile. All grid cells where the percentage is greater than expected by chance are shaded and grid cells where the percentage is significantly greater than expected by chance at the 5% level are highlighted.

use temperature extreme index values based on monthly counts of daily exceedances, while this study uses the top and bottom 10% of the daily and monthly temperature distribution. The percentage anomalies in both studies are relatively small for many locations (generally within 5%–10% of the expected value), but they can be statistically significant when the sample size is larger although not significant according to the Monte Carlo tests employed in this study. In addition to the shorter time period used in this work, the 30-yr period used here may influence the diagnosed relationship between extremes and ENSO. The weak association percentages and the large number of extreme days that occur when ENSO is not in the upper or lower quartile of index values suggests that ENSO is not a dominant influence on extremes at this time scale and during the 30-yr period used in this analysis.

3) INDIVIDUAL CASES

Individual locations were chosen to more closely examine the interaction between temperature extremes and the modes of variability. Here we present results from four locations represented by grid cells located in Alaska, the U.S. central Gulf Coast, Baffin Island, and the Great Lakes. Extreme temperatures at the Alaska location are strongly influenced by the PNA and to a lesser extent ENSO. Extremes in the vicinity of the Gulf Coast are influenced by the PNA and the NAM while Baffin Island is affected by the NAM and the Great Lakes is an example of a location not within a major region of influence from any mode. The Alaska, Gulf Coast, and Baffin Island cases are examples of associations that are stronger than the majority of the continent while results from the Great Lakes location are more representative of areas outside of the main regions of influence from these patterns.

Figure 5 shows the index values for all extreme DJF and JJA days and months at the four locations using a box-and-whisker format with each dot representing one extreme temperature day/month. For the daily case, a large spread of index values, regardless of association value or significance, is evident for both modes. Locations where the boxes (outlining the days/months between the 25th and 75th percentile) do not overlap are indicative of cases where the association with temperature is relatively strong. Some notably strong associations with daily extremes, such as Baffin Island with the NAM and Alaska with the PNA in winter, do not have overlap between the boxes while there is still substantial overlap between the dots. These areas of relatively strong association also have extremes occurring during the opposite phase of preferred association.

The Baffin Island case exhibits some asymmetry as the NAM values for daily Tx90 deviate from zero in the negative direction with greater magnitude (median −1.5) than the values for daily Tn10 (median 0.14) in the positive direction. Only the Baffin Island daily Tx90 NAM case and the Alaska daily Tx90 and Tn10 PNA cases have boxes that fall entirely within one phase of the mode. This ubiquitous spread in daily cases further indicates that extreme daily temperatures are strongly influenced by mechanisms other than the phase and strength of these modes of variability, even where the NAM and PNA are highly influential on mean temperature or significantly associated with extreme temperature in a statistical sense.

Monthly extremes show less overlap between boxes and, in the cases of Baffin Island with the NAM and Alaska with the PNA, there is no overlap between extreme months. There is a greater tendency toward a positive phase of the NAM for Baffin Island with monthly than daily Tn10, but the deviation from zero is still higher for monthly Tx90, indicating some asymmetry at monthly time scales as well. The Gulf Coast location shows strong tendencies toward opposing phases of the NAM and the PNA for extreme months while this is not the case for daily extremes. The Great Lakes location also shows association with the phase of the NAM that is not present with daily extremes. This suggests that the influence from the NAM on temperature at this location is present at monthly time scales while other mechanisms are more important for daily extremes. Plotted in the same manner, JJA box-and-whisker plots show little or no tendency toward either positive or negative phases of either mode for daily or monthly extremes.

The scatterplots in Fig. 6 illustrate the relationship between minimum temperature and index value for every day in the 30-yr climatology at Baffin Island and Alaska in DJF and maximum temperature for JJA. These are two places where the associations are among the strongest in the continent for both daily and monthly extremes, especially in winter; however, the daily scatterplots show many extreme DJF days that occur when the modes are not in a NAM± or PNA± state. Overall, there is a relationship between temperature and the phase and strength of the modes as indicated by the slope of the scatterplot, but even locations with the strongest associations in North America still have many extreme days occurring outside of the index value threshold and in some cases during phases opposite in sign to the preferred phase of association.

The Baffin Island daily DJF scatterplot illustrates the asymmetry seen in the box-and-whisker plots. The temperature probability density function for this region (not shown) has a long warm tail, largely associated with a negative phase of the NAM, which allows advection of

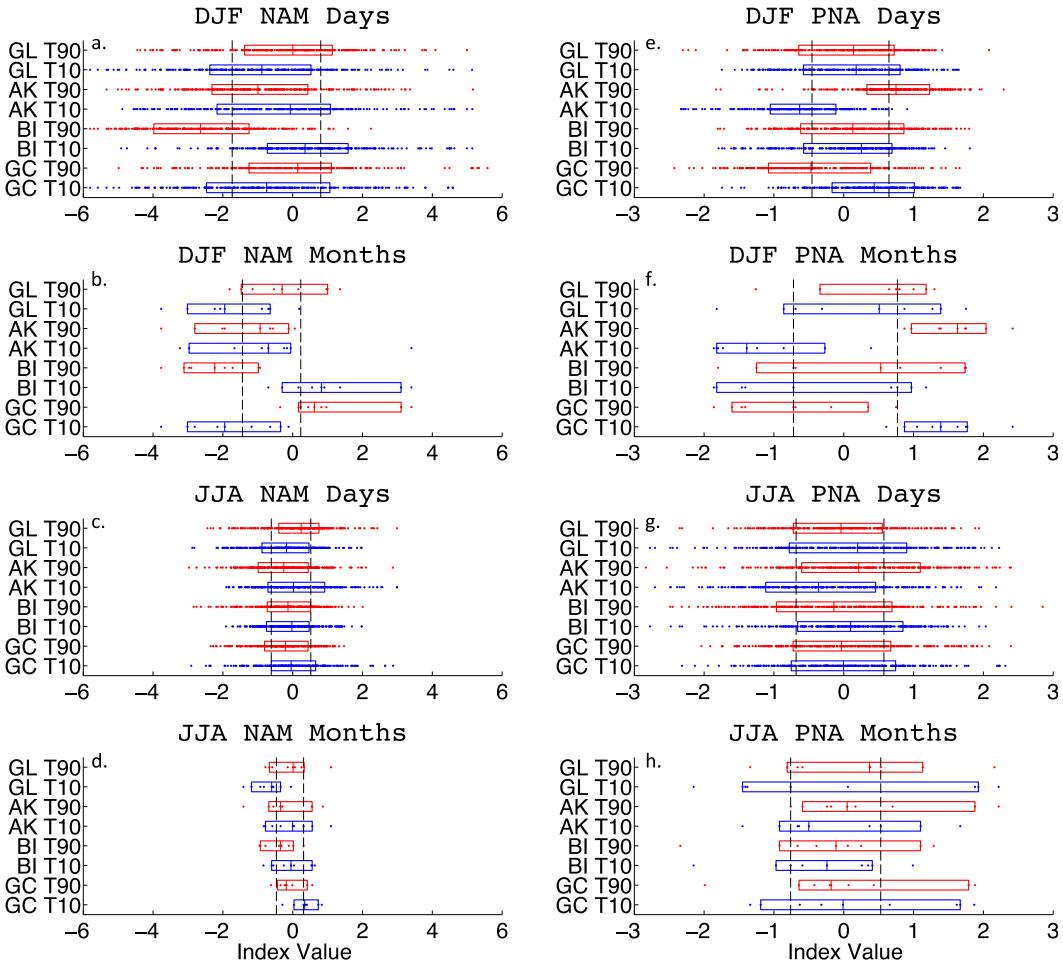

FIG. 5. Box-and-whisker plots showing the (a)–(d) NAM and (e)–(h) PNA index values concurrent with cold (blue) and warm (red) extreme minimum DJF temperature (a),(e) days and (b),(f) months and extreme warm maximum JJA temperature (c),(g) days and (d),(h) months. Each dot represents one extreme temperature day/month. The box outlines the 25th and the 75th percentiles of index values for that location while the vertical line in the box marks the median. The black vertical lines delineate the lower and upper quartiles of the index values for all days or months for reference with Fig. 1. The locations are the Great Lakes (GL), Alaska (AK), Baffin Island (BI), and the Gulf Coast (GC).

relatively mild marine air from the south and southeast into this relatively cold location. Days in the cold tail are less associated with a preferred mechanism that can cause outbreaks of equally cold air because this location is already in close proximity to the climatologically coldest regions in the hemisphere.

Monthly scatterplots for DJF are narrower in shape and have few extreme months occurring during an opposing sign from the preferred association than for the daily case. In the daily case there is a higher proportion of Tn10 days falling outside of NAM+ days and even some occurring with NAM− days, than in the monthly case. This is also true for the PNA Alaska case as very few months occur with an index value that is outside of the expected phase. The longer time scale increases the association in these two places in a manner consistent with the difference between the daily and monthly percentage values depicted in Figs. 1 and 2. In contrast, JJA daily and monthly scatterplots show weak association compared with DJF in all cases, consistent with the findings in section 2.

To summarize the results shown in Figs. 4–6, Table 1 shows the odds of having an extreme temperature concurrent with days in the upper quartile of the NAM or PNA versus days in the lower quartile at select locations. For example, if 50% of extreme temperature days occur when the NAM is in the upper quartile of the index distribution and 25% occur when the NAM is in the lower quartile of the distribution, the ratio would be 2, meaning it is twice as likely to have an extreme

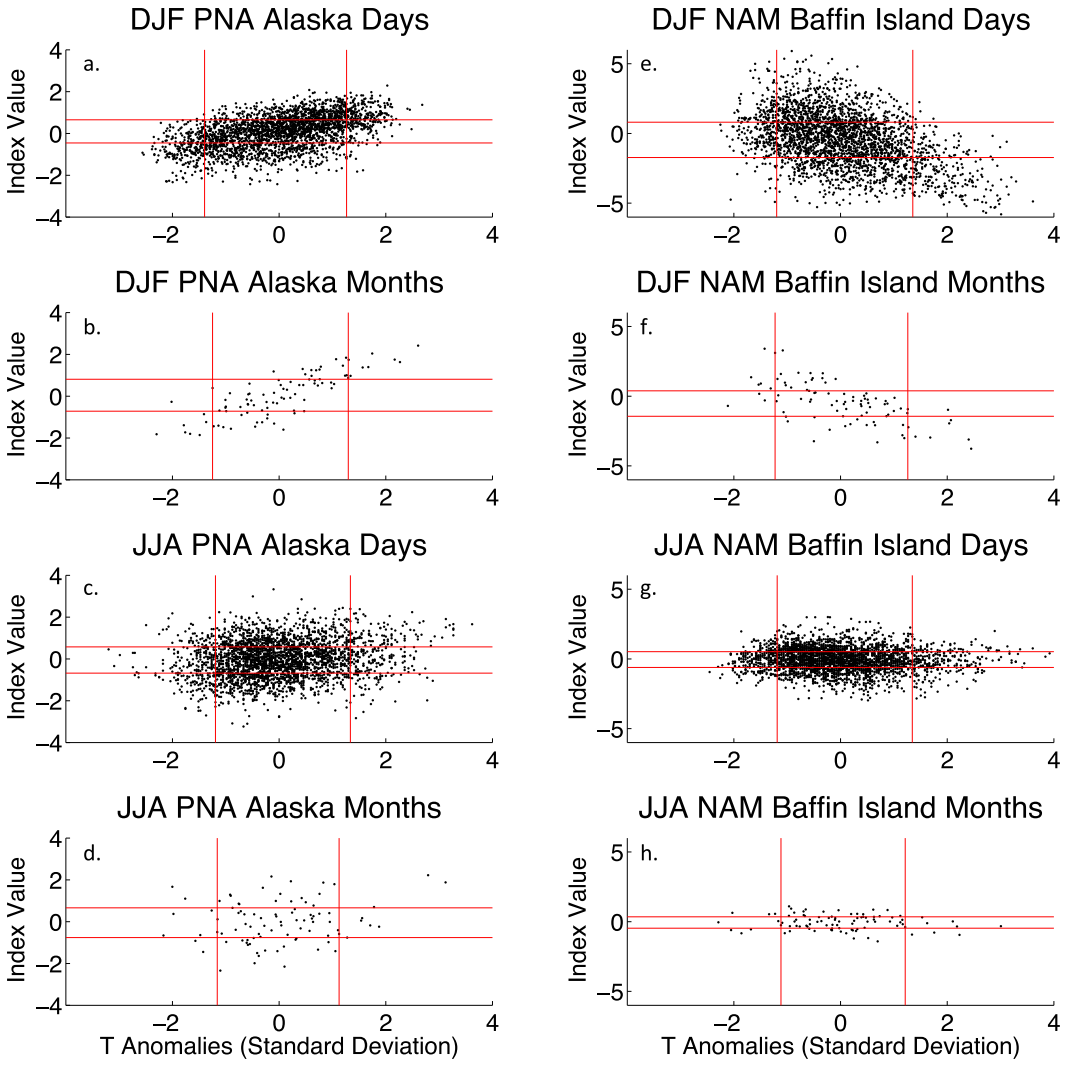

FIG. 6. Scatterplots of normalized (a),(b),(e),(f) minimum DJF and (c),(d),(g),(h) maximum JJA temperature anomalies vs index values of the (left) PNA for Alaska and (right) the NAM for Baffin Island. The vertical red lines indicate the 10th and 90th percentile of temperature anomalies and the horizontal red lines indicate the 25th and 75th percentile of the index values.

temperature when the NAM is in the upper quartile as it is in the lower. Baffin Island shows the greatest odds with Tn10 days being 5.8 times more likely when the NAM is in the upper than the lower quartile while Alaska shows almost no Tn10 days occurring when the PNA is in the upper quartile of the distribution.

Figure 7 shows scatterplots for ENSO DJF minimum and JJA maximum temperature associations at the Gulf Coast and Alaska locations, which are both in regions known to be influenced by ENSO teleconnections. These are locations where the associations with ENSO are expected to be stronger than for the majority of the continent. Daily DJF temperatures show very little relationship with the sign and strength of the Niño-3.4 index while there is a somewhat stronger relationship with monthly temperature. In comparison with the scatterplots for the NAM and PNA, the relationships are notably weak with ENSO in these two locations. There is a tendency for extreme warm months to be associated with La Niña events in the Gulf Coast region with a weaker tendency for extreme cold events to be associated with El Niño events in winter. In JJA, the association is also weak for daily and monthly extremes at the Gulf Coast location, while some association is seen between ENSO and daily and monthly extremes at the Alaska location. These scatterplots help illustrate the weak influence ENSO has on the tails of the temperature distribution over North America

TABLE 1. Ratio of extreme temperature days concurrent with days in the upper quartile to those concurrent with days in the lower quartile of the NAM and PNA. All extremes are Tn10 for DJF and Tx90 for JJA. A value of 1 would mean that the odds of having an extreme temperature are the same for both quartiles of the circulation pattern.

	NAM	PNA
DJF Tn10 Gulf Coast	0.75	3.4
DJF Tn10 Alaska	1.1	0.01
DJF Tn10 Baffin Island	5.8	0.94
DJF Tn10 Great Lakes	0.51	1.1
JJA Tx90 Gulf Coast	1.2	1.1
JJA Tx90 Alaska	1.4	0.47
JJA Tx90 Baffin Island	0.86	1.5
JJA Tx90 Great Lakes	0.67	1.3

and suggest that other mechanisms are substantially more important for the occurrence of extreme temperatures especially on daily time scales in the cases examined here.

4. Dependence of circulation patterns on time scale

In LB12, composite analysis was used to identify and describe the concurrent circulation anomaly patterns in sea level pressure (SLP) and 500-hPa geopotential height (Z_{500}) associated with temperature extremes over North America. To determine if the resulting circulation patterns are dependent on time scale, composite patterns were computed for a longer period centered on the day of the extreme temperature day. Figure 8 shows composite anomalies for Z_{500} for the day of the extreme (labeled ±0) and for a 15-day period centered on the day of the extreme (labeled ±7), and Fig. 9 shows composite anomalies for extreme temperature months. All DJF plots are for extreme cold minimum temperature days and all JJA plots are for extreme warm maximum temperature days or months.

The ±0 composites for cold minimum temperature days in DJF show robust negative Z_{500} height anomalies nearby or downstream of the location with weaker positive anomalies upstream. The pattern of height anomalies resembles the characteristic wave train associated with the positive phase of the PNA for the Gulf Coast example and the negative phase of the PNA for the Alaska example. When the composite includes the entire 15-day period centered on the extreme day, the local anomaly center weakens in greater proportion to the anomaly centers farther away while maintaining the PNA-like wave train. A disproportional weakening of the local anomaly center in relation to the more remote anomalies is suggestive of the larger-scale teleconnection pattern playing an important role as local synoptic-scale weather events are averaged out. The local anomaly pattern in the ±0-day composites can therefore be considered a combination of a larger-scale circulation pattern like the NAM or PNA and local weather that contribute together to cause an extreme temperature day. In the Alaska and Gulf Coast cases, the PNA may act as an important factor in the occurrence of extreme temperature days, but local weather plays a role in determining which specific days breach the 10% temperature threshold.

A similar result is seen at Baffin Island, except with the positive phase of the NAM in this case. The Great Lakes example exhibits some commonalities with the negative phase of the NAM but with a very strong weakening of the local negative anomaly center; weather likely plays a strong role in this region. Here, influence from the NAM or other modes of variability is weaker than in the other cases, which helps explain the larger dependency on transient synoptic-scale circulation that is important here. SLP anomaly composites (not shown) further support the hypothesis that a local weather pattern being superimposed on a teleconnection pattern is typically associated with extreme temperature days in these locations.

In JJA, Z_{500} anomalies are weaker, especially at the two midlatitude locations (Gulf Coast and Great Lakes). The weakening of the anomalies in the ±7-day cases is more proportional between all anomaly centers. While this is subtle, it is consistent with a summertime pattern that is dominated by local, smaller-scale circulation that often persists for time scales shorter than 15 days. At higher latitudes, as in the Alaska and Baffin Island cases, strong anomalies are still present even in the ±7-day case. Here the atmosphere is relatively baroclinic in summer when compared with lower latitudes, so large-scale circulation patterns that evolve over long time periods are still common. These results support the lower association percentages seen in JJA and are consistent with the overall weaker atmospheric circulation in the Northern Hemisphere summer months.

The composites of monthly mean Z_{500} anomalies shown in Fig. 9 more closely resemble the characteristic circulation patterns associated with the NAM and PNA. In winter, the composite pattern for Tn10 months resembles both the PNA+ and the NAM− patterns for the Gulf Coast location. The Alaska location has a composite pattern resembling PNA− for Tn10 and PNA+ for Tn90. The composite pattern for Baffin Island resembles NAM+ for Tn10 months and NAM− for Tn90 months. The Great Lakes location has some commonalities with NAM− and PNA+ for Tn10 while the Tn90 composite pattern does not strongly resemble either pattern. JJA patterns are weak and generally

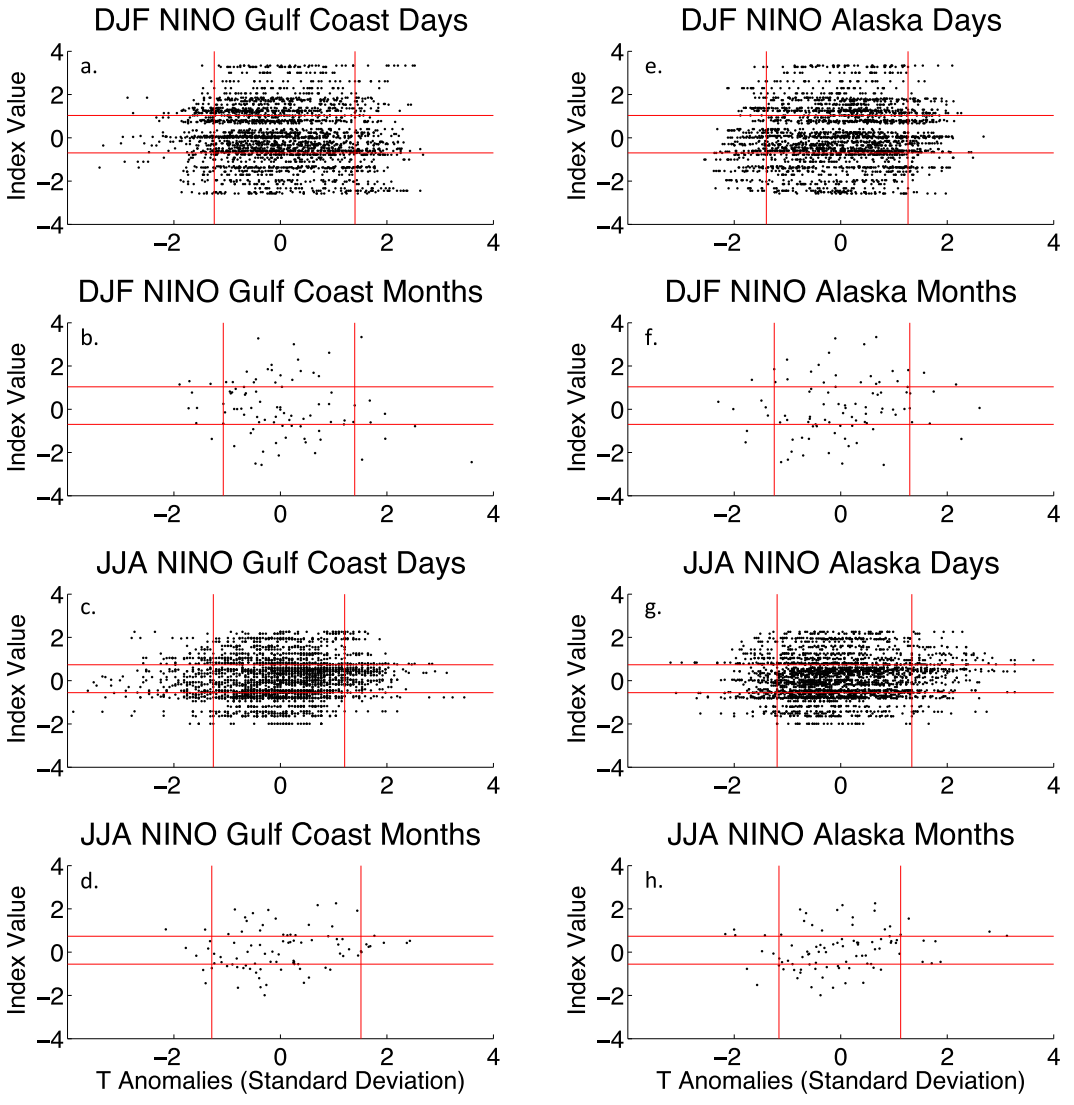

FIG. 7. As in Fig. 6, but for Niño-3.4 at the (a)–(d) Gulf Coast and (e)–(h) Alaska locations.

localized for extreme months. These results further illustrate the greater influence the NAM and PNA have on extreme temperatures on monthly time scales compared with daily and on winter extremes compared with summer.

5. Soil moisture influences

The weaker association percentages and lack of evidence of large-scale circulation patterns in JJA lead to the question: if large-scale, recurrent modes of climate variability are not highly associated with extreme temperatures in the summer, what other mechanisms are important? One possible mechanism is anomalous near-surface soil moisture content. To test the hypothesis that extreme temperatures in summer are strongly associated with anomalous soil moisture, Fig. 10 shows the association percentages between extreme warm JJA maximum and minimum temperature days and extremely dry soil moisture (lower quartile of days) and extreme cool JJA maximum and minimum temperature days with unusually moist soil (upper quartile of days).

In almost all locations, extreme warm maximum temperature days have a higher probability of occurring when soil moisture is unusually low. This is consistent with the expected association as dry soil can enhance surface temperatures because of decreased evaporation and evapotranspiration and has been associated with extreme heat episodes, like the European heat wave of 2003 (e.g., Fischer et al. 2007). Extreme warm minimum temperature days are less associated with unusually dry conditions. Because minimum temperatures occur

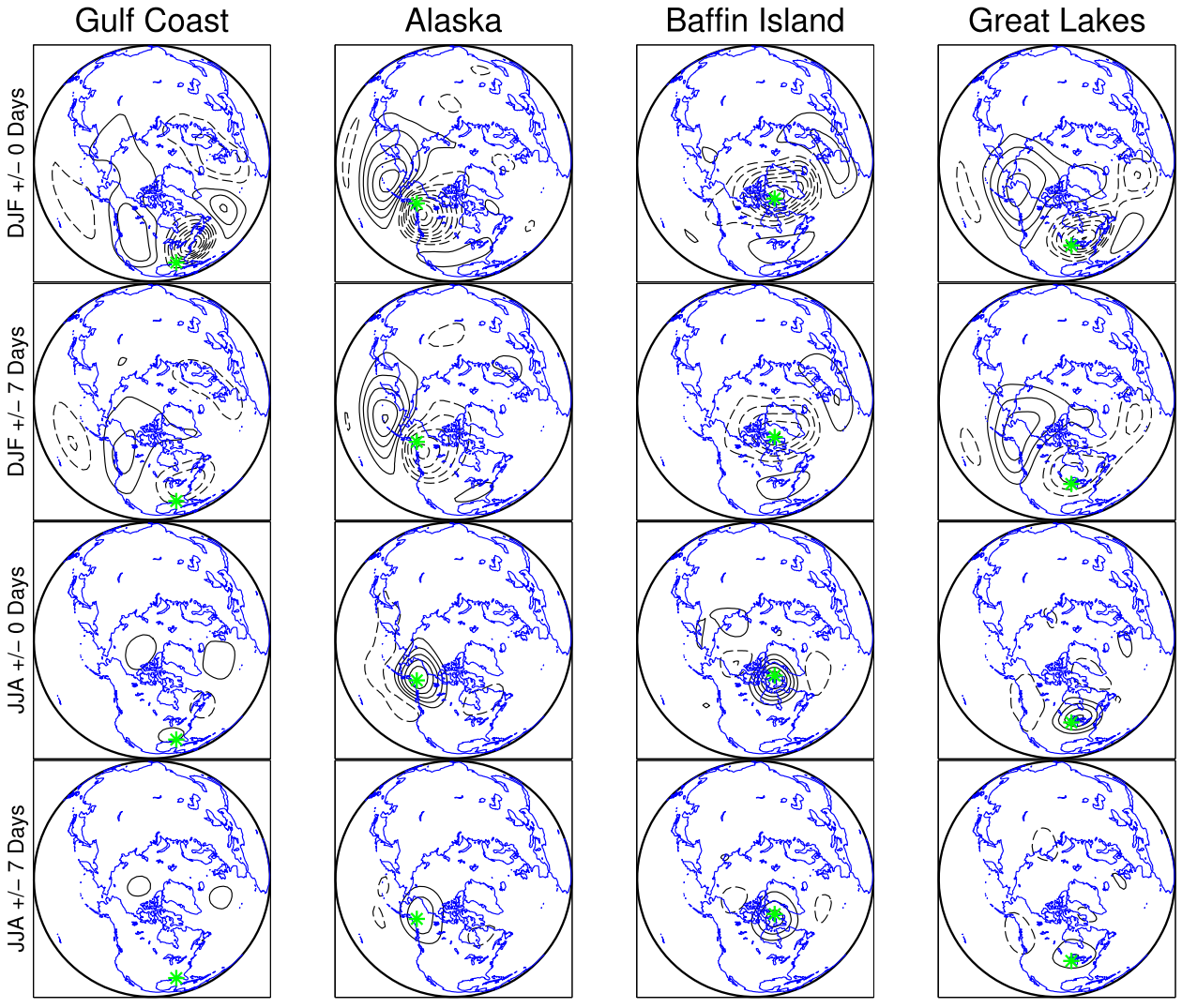

FIG. 8. Composites of Z_{500} anomalies for all extreme cold DJF minimum temperature days and all extreme warm JJA maximum temperature days for each of the four locations that are centered on the green star. Negative (positive) anomalies are contoured with dashed (solid) lines. The contour interval is 20 m and the zero contour is omitted. Rows labeled as ±0 days are composites of anomalies for only the extreme temperature days, while rows labeled as ±7 days are composites of the 15-day mean anomaly centered on the extreme temperature day.

during the night when there is no insolation, dry surface conditions would not be expected to enhance heating or inhibit cooling, all other things being equal. Areas where there is a significant increase in the probability of extremely warm nights when soil moisture is low may be due to residual extreme daytime heat that was influenced by dry surface conditions.

Similar to the enhancement effect on surface temperature that unusually dry surface conditions have, unusually wet soil can inhibit surface heating during the daytime. There is a strong association between extremely cool JJA maximum temperatures and unusually moist soil over the western half of the United States with weaker but still significant associations along the Gulf Coast. This association could indicate that unusually moist surface conditions inhibit daytime warming, but it could also suggest that weather patterns that cause precipitation in this region decrease the temperature through cloudiness or evaporative cooling of the lower atmospheric column by precipitation. The same association is not seen in extreme cold minimum JJA temperatures where unusually moist surface conditions can inhibit diurnal cooling. Additionally, if wet days are associated with cloudiness, this could also inhibit nighttime radiational cooling. Analysis of soil moisture as a precursor to extreme temperatures was also performed (not

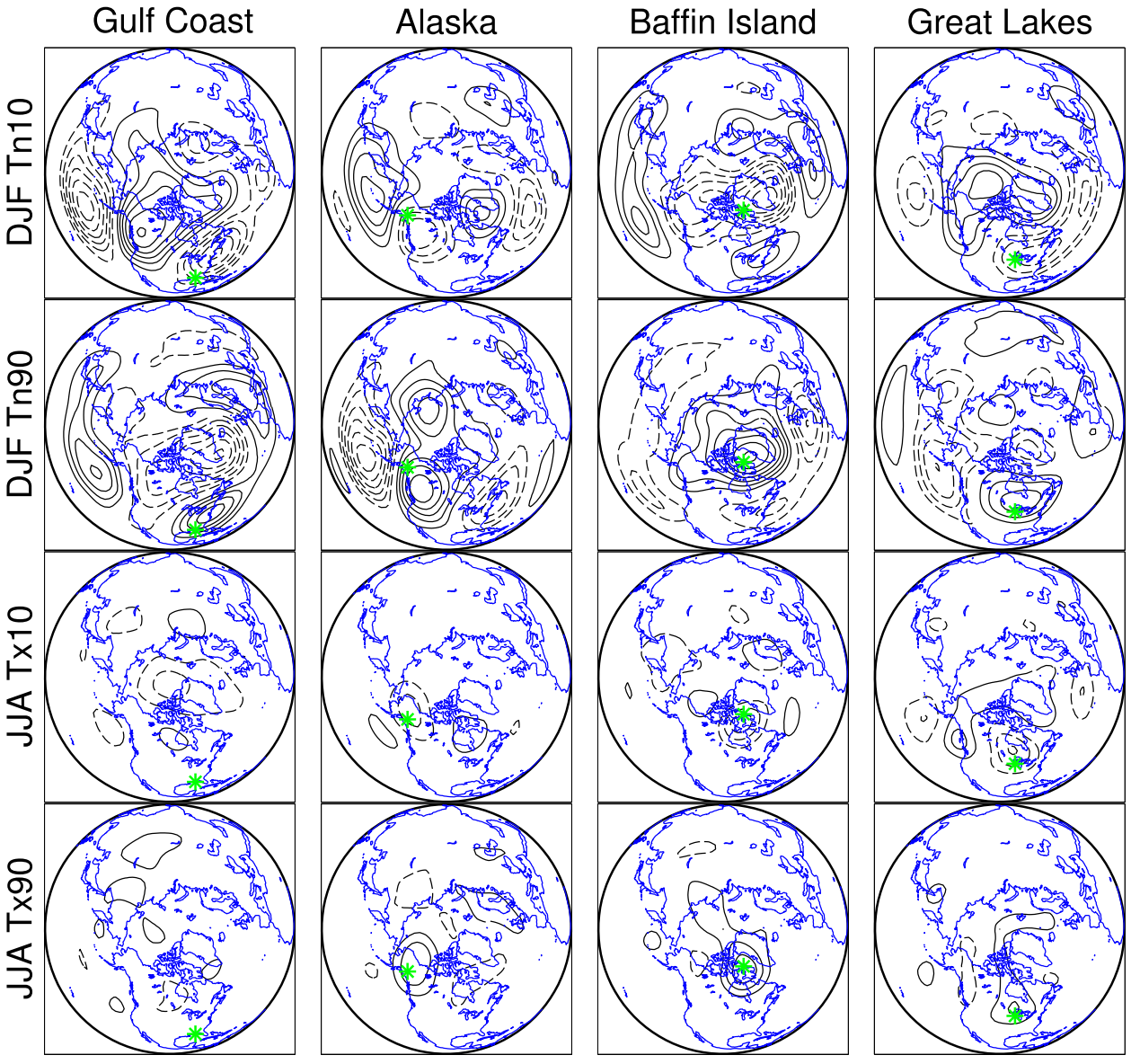

FIG. 9. Composite of Z_{500} anomalies for extreme temperature months. From top to bottom, DJF extreme cold minimum temperature months, DJF extreme warm minimum temperature months, JJA extreme cold maximum temperature months, and JJA extreme warm maximum temperature months; columns and contours as in Fig. 8.

shown) with results resembling those of coincident soil moisture but with overall weaker association values. This suggests that soil moisture may be important on both long and short temporal scales.

While unusually dry soil appears to influence extreme warm daytime high temperatures uniformly across the domain, the western United States has a greater association between unusually wet soil and extremely cool daytime maximum temperatures. Such conditions in the relatively arid western United States increase latent heat flux proportionately more than unusually moist conditions in the climatologically humid eastern United States. This increase in latent heat flux and decrease in sensible heat flux relative to climatology could also result in the higher association between unusually wet soil and extreme cool summer maximum temperatures here.

6. Summary and concluding remarks

The influence of the PNA, NAM, and ENSO on extreme temperature days and months for North American winters and summers is quantified. These results suggest that the PNA and NAM play important roles in the occurrence of extreme temperature days in the

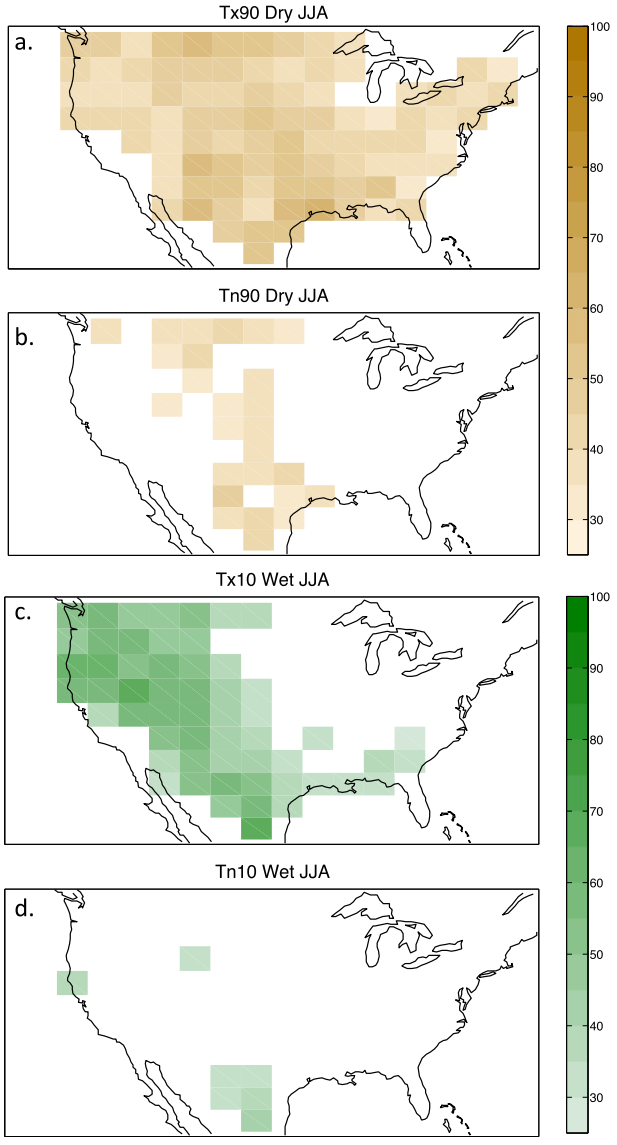

FIG. 10. Percentage of extremely warm JJA (a) maximum and (b) minimum temperature days that occurred when soil moisture was in the driest quartile of days at each grid cell and extremely cold (c) maximum and (d) minimum temperature days that occurred when the soil moisture was in the wettest quartile of days at each grid cell.

regions in the vicinity of the characteristic atmospheric circulation anomalies associated with these modes of variability. Many extreme temperature events also occur when an influential mode of variability is not in the preferred phase and in some cases is opposite in sign from the preferred phase. More extreme temperature days are influenced by the PNA than the NAM over the continent in winter than in summer. Areas in northwestern North America are strongly influenced by the PNA while the PNA affects southeastern North America in the opposite way in wintertime. The NAM is also particularly influential over the northeastern parts of the continent and in a band running from the northwestern to southeastern parts of North America in winter. Few locations have an increased probability of extreme temperatures when neither the PNA nor the NAM are unusually positive or negative in the winter while numerous extreme warm days occur when neither pattern is outside of the upper or lower quartiles of the index value distribution in the summer. In general, summertime associations with both modes are weaker and less systematic than wintertime associations.

Local, transient, synoptic-scale weather patterns are also key to causing a given day to have an extreme temperature in most locations, but this is often in conjunction with an unusually strong phase of an influential mode of climate variability. Composite analysis of anomalies in SLP and Z_{500} at four locations illustrate the dominance of the PNA and NAM in the areas of influence for these patterns while also showing that synoptic-scale weather patterns superimposed on these larger-scale teleconnection patterns are present. Summertime associations are weaker and largely limited to higher latitudes where large-scale circulation is more dominant compared with the less baroclinic atmosphere farther south.

Association between ENSO and extreme temperature days tends to be weak in the analysis performed in this work. There is a slight increase in significant association between ENSO and extreme temperature months. While ENSO can have an impact on local temperature, these results suggest that other mechanisms are substantially more important for the occurrence of extremes in both winter and summer. Because ENSO is defined by SST anomalies in the equatorial Pacific Ocean, it follows that associations would be weaker over North America than in the cases of the PNA and NAM, which are defined by atmospheric circulation anomalies with centers of action over the continent.

It is also possible that variability in the characteristics of an ENSO event has an impact on the type and strength of the associated impacts on extremes. For example, two different types of El Niño events have been identified, each with different temperature teleconnections over North America. The traditional warm event is characterized by warm sea surface temperature anomalies centered over the eastern tropical Pacific (EP) while the other type is centered over the central tropical Pacific (CP) (Yu et al. 2012, and references therein). The CP events are associated with a temperature anomaly dipole with warm anomalies over the northwestern United States and cold anomalies over the southeastern United States. The EP events are characterized by warm anomalies primarily

over the northern tier of the United States. Because these two varieties of ENSO events influence mean temperature differently, it follows that these two varieties influence temperature extremes differently also.

Anomalous soil moisture, affecting the local surface energy budget, is influential in many cases for the occurrence of extremes in summer. Over the continental United States, extreme warm summer days tend to be associated with unusually dry surface soil moisture and extreme cool days are often associated with unusually moist soil moisture (especially in the western United States). A more comprehensive analysis of mechanisms that affect the surface radiation balance in summer months would help identify other important mechanisms and their causes for summer extremes.

Acknowledgments. This study was supported by the Office of Science (BER), U.S. Department of Energy, Award DE-SC0005467. We thank John Lanzante for his insight and extremely helpful advice during this work. We also thank Justin Sheffield for providing the VIC data. This work was done as a private venture and not in the author's capacity as an employee of the Jet Propulsion Laboratory, California Institute of Technology.

REFERENCES

Alexander, L. V., and Coauthors, 2006: Global observed changes in daily climate extremes of temperature and precipitation. *J. Geophys. Res.,* **111,** D05109, doi:10.1029/2005JD006290.

Barnston, A. G., and R. E. Livezey, 1987: Classification, seasonality, and persistence of low-frequency atmospheric circulation patterns. *Mon. Wea. Rev.,* **115,** 1083–1126.

Beniston, M., 2004: The 2003 heat wave in Europe: A shape of things to come? An analysis based on Swiss climatological data and model simulations. *Geophys. Res. Lett.,* **31,** L02202, doi:10.1029/2003GL018857.

Brown, P. J., R. S. Bradley, and F. T. Keimig, 2010: Changes in extreme climate indices for the Northeastern United States, 1870–2005. *J. Climate,* **203,** 6555–6572.

Caesar, J., L. Alexander, and R. Vose, 2006: Large-scale changes in observed daily maximum and minimum temperatures: Creation and analysis of a new gridded data set. *J. Geophys. Res.,* **111,** D05101, doi:10.1029/2005JD006280.

Cattiaux, J., R. Vautard, C. Cassou, P. Yiou, V. Masson-Delmotte, and F. Codron, 2010: Winter 2010 in Europe: A cold extreme in a warming world. *Geophys. Res. Lett.,* **37,** L20704, doi:10.1029/2010GL044613.

Christidis, N., P. A. Stott, S. Brown, G. Hegerl, and J. Caesar, 2005: Detection of changes in temperature extremes during the second half of the 20th century. *Geophys. Res. Lett.,* **32,** L20716, doi:10.1029/2005GL023885.

——, ——, and ——, 2011: The role of human activity in the recent warming of extremely warm daytime temperatures. *J. Climate,* **24,** 1922–1930.

Dole, R., and Coauthors, 2011: Was there a basis for anticipating the 2010 Russian heat wave? An analysis based on Swiss climatological data and model simulations. *Geophys. Res. Lett.,* **38,** L06702, doi:10.1029/2010GL046582.

Fischer, E. M., S. I. Seneviratne, P. L. Vidale, D. Lüthi, and C. Schär, 2007: Soil moisture–atmosphere interactions during the 2003 European summer heat wave. *J. Climate,* **20,** 5081–5099.

Frich, P., V. Alexander, P. Della-Marta, B. Gleason, M. Haylock, A. M. G. Klein Tank, and T. Peterson, 2002: Observed coherent changes in climatic extremes during the second half of the twentieth century. *Climate Res.,* **19,** 193–212.

Gershunov, A., and T. P. Barnett, 1998: ENSO influence on intraseasonal extreme rainfall and temperature frequencies in the contiguous United State: Observations and model results. *J. Climate,* **11,** 1575–1586.

Griffiths, M. L., and R. S. Bradley, 2007: Variations of twentieth-century temperature and precipitation extreme indicators in the northeast United States. *J. Climate,* **20,** 5401–5417.

Guirguis, K., A. Gershunov, R. Schwartz, and S. Bennett, 2011: Recent warm and cold daily winter temperature extremes in the Northern Hemisphere. *Geophys. Res. Lett.,* **38,** L17701, doi:10.1029/2011GL048762.

Higgins, R. W., A. Leetmaa, and V. E. Kousky, 2002: Relationships between climate variability and winter temperature extremes in the United States. *J. Climate,* **15,** 1555–1572.

Horel, J. D., and J. M. Wallace, 1981: Planetary-scale atmospheric phenomena associated with the Southern Oscillation. *Mon. Wea. Rev.,* **109,** 813–829.

Hurrell, J. W., Y. Kushnir, G. Ottersen, and M. Visbeck, 2003: An overview of the North Atlantic Oscillation. *The North Atlantic Oscillation: Climate Significance an Environmental Impact, Geophys. Monogr.,* Vol. 134, Amer. Geophys. Union, 1–35.

Kalnay, E., and Coauthors, 1996: NCEP/NCAR 40-Year Reanalysis Project. *Bull. Amer. Meteor. Soc.,* **77,** 437–471.

Kenyon, J., and G. C. Hegerl, 2008: Influence of modes of climate variability on global temperature extremes. *J. Climate,* **21,** 3872–3889.

Kiladis, G. N., and H. F. Diaz, 1989: Global climatic anomalies associated with extremes in the Southern Oscillation. *J. Climate,* **2,** 1069–1090.

Kodra, E., K. Steinhaeuser, and A. R. Ganguly, 2011: Persisting cold extremes under 21st-century warming scenarios. *Geophys. Res. Lett.,* **38,** L08705, doi:10.1029/2011GL047103.

Liang, X., D. P. Lettenmaier, E. F. Wood, and S. J. Burges, 1994: A simple hydrologically based model of land surface water and energy fluxes for GSMs. *J. Geophys. Res.,* **99** (D7), 14 415–14 428.

Loikith, P. C., and A. J. Broccoli, 2012: Characteristics of observed atmospheric circulation patterns associated with temperature extremes over North America. *J. Climate,* **25,** 7266–7281.

Meehl, G. A., and C. Tebaldi, 2004: More intense, more frequent, and longer lasting heat waves in the 21st century. *Science,* **305,** 994–997.

——, and Coauthors, 2007: Global climate projections. *Climate Change 2007: The Physical Science Basis,* S. Solomon et al., Eds., Cambridge University Press, 747–846.

——, C. Tebaldi, G. Walton, D. Easterling, and L. McDaniel, 2009: Relative increase of record high maximum temperatures compared to record low minimum temperatures in the U.S. *Geophys. Res. Lett.,* **36,** L23701, doi:10.1029/2009GL040736.

Morak, S., G. C. Hegerl, and J. Kenyon, 2011: Detectable regional changes in the number of warm nights. *Geophys. Res. Lett.,* **38,** L17703, doi:10.1029/2011GL048531.

——, ——, and N. Christidis, 2013: Detectable changes in the frequency of temperature extremes. *J. Climate,* **26,** 1561–1574.

Quadrelli, R., and J. M. Wallace, 2004: A simplified linear framework for interpreting patterns of Northern Hemisphere wintertime climate variability. *J. Climate,* **17,** 3728–3744.

Rahmstorf, S., and D. Coumou, 2011: Increase of extreme events in a warming world. *Proc. Natl. Acad. Sci. USA,* **108,** 17 905–17 909, doi:10.1073/pnas.1101766108.

Ropelewski, C. F., and M. S. Halpert, 1987: Global and regional scale precipitation patterns associated with the El Nino/Southern Oscillation. *Mon. Wea. Rev.,* **115,** 1606–1626.

Schär, C., P. L. Vidale, D. Lüthi, C. Frei, C. Häberli, M. A. Liniger, and C. Appenzeller, 2004: The role of increasing temperature variability in European summer heatwaves. *Nature,* **427,** 332–336.

Stott, P. A., D. A. Stone, and M. R. Allen, 2004: Human contribution for the European heatwave of 2003. *Nature,* **432,** 610–614.

Straus, D. M., and J. Shukla, 2002: Does ENSO force the PNA? *J. Climate,* **15,** 2340–2358.

Tebaldi, C., K. Hayhoe, J. M. Arblaster, and G. A. Meehl, 2006: Going to the extremes, an intercomparison of model-simulated historical and future changes in extreme events. *Climatic Change,* **79,** 185–211.

Thompson, D. W. J., and J. M. Wallace, 1998: The Arctic Oscillation signature in the wintertime geopotential height and temperature fields. *Geophys. Res. Lett.,* **25,** 1297–1300.

——, and ——, 2000: Annular modes in the extratropical circulation. Part I: Month-to-month variability. *J. Climate,* **13,** 1000–1016.

——, and ——, 2001: Regional climate impacts of the Northern Hemisphere annular mode. *Science,* **293,** 85–89.

Trenberth, K. E., 1997: The definition of El Niño. *Bull. Amer. Meteor. Soc.,* **78,** 2771–2777.

Vavrus, S., J. E. Walsh, W. L. Chapman, and D. Portis, 2006: The behavior of extreme cold air outbreaks under greenhouse warming. *Int. J. Climatol.,* **26,** 1133–1147.

Wallace, J. M., and D. S. Gutzler, 1981: Teleconnections in the geopotential height field during the Northern Hemisphere winter. *Mon. Wea. Rev.,* **109,** 784–812.

Wang, C., H. Liu, and S.-K. Lee, 2010: The record-breaking cold temperatures during the winter of 2009/2010 in the Northern Hemisphere. *Atmos. Sci. Lett.,* **11,** 161–168.

Wettstein, J. J., and L. O. Mearns, 2002: The influence of the North Atlantic–Arctic Oscillation on mean, variance, and extremes of temperature in the northeastern United States and Canada. *J. Climate,* **15,** 3586–3600.

Yu, J.-Y., Y. Zou, S. T. Kim, and T. Lee, 2012: The changing impact of El Niño on US winter temperatures. *Geophys. Res. Lett.,* **39,** L15702, doi:10.1029/2012GL052483.

Zwiers, F. W., X. Zhang, and Y. Feng, 2011: Anthropogenic influence on long return period daily temperature extremes at regional scales. *J. Climate,* **24,** 881–892.